# ROLE OF CONNCECTED MEMBERS ON THE LOAD BEARING CAPACITY OF COMPRESSED RC COLUMNS - VALIDATION OF CONSTEEL'S METHOD



https://doi.org/10.32970/CS.2024.1.1

Szabolcs Szinvai - Bálint Vaszilievits-Sömjén - Tamás Kovács

*Reinforced concrete (RC) columns are crucial in construction, yet their design is challenging. Design typically involves first-order analysis, consideration of imperfections, and calculation of second-order effects, often done on an isolated column for simplicity, without precise consideration of adjacent elements. Although this approach is generally effective, it can lead to serious errors in certain cases. To investigate this problem, single columns under axial compression with different support conditions were first evaluated, followed by two columns connected by a stiff beam with hinged connections. The columns studied were either loaded at different intensities, had different boundary conditions, or had different cross-sectional areas. The evaluations included the nominal curvature method; the automatic nominal curvature method in ConSteel, which is a novel approximation of the second-order bending moments based on buckling shapes; and the general method. The results showed that if there is a significant difference in stiffness or in loading intensity between the connected members, the nominal curvature method can underestimate the bending moments compared to the general method. Therefore, in the case of irregular structures, more precise consideration of adjacent elements during design is essential to ensure safety. It was shown that this can be done automatically using the automatic nominal curvature method in ConSteel.*

**Keywords:** second-order effects, nonlinear analysis, column, interaction

## 1. INTRODUCTION

In contemporary architectural design, slender columns are increasingly favoured due to their efficiency in material use and their ability to enhance spatial utility within interiors. These slender, compressed structural members are susceptible to pronounced second-order effects and require careful evaluation.

The Eurocode 2 standard (EN 1992-1-1, 2004) allows the application of three methodologies for the computation of second-order effects. The nominal curvature (NC) and nominal stiffness (NS) methods are prevalently employed by designers. These approaches are characterised by their simplified and deterministic nature.

The third approach is the general nonlinear method (GM), which is regarded as a more precise design strategy and considered one of the most accurate methodologies available. However, this method is rendered impractical due to its inherent complexity and the challenges it poses in practical application.

The nominal curvature and nominal stiffness approaches give significantly different results. The applicability of the nominal stiffness approach is limited to scenarios where the design load is considerably lower than the buckling load or where the column exhibits minimal slenderness (Araújo, 2017). However, the nominal curvature approach also provides effective results for slender columns. This method uses the slenderness ratio. In cases where the column has marginal slenderness in a particular direction, second-order effects may be disregarded in that direction. This makes it easier to deal with different types of columns.

Many software applications have incorporated these two simplified solutions. Certain applications have implemented these methods with a high degree of precision, adhering strictly to the Eurocode standards. In contrast, other applications have attempted to exploit computational capabilities either by extending the simplified methods or by using a variant of the GM method.

As the construction of increasingly large and more complex structures becomes more prevalent, so does the reliance on automated software solutions. These solutions must be able to address imperfections and second-order effects. A significant advantage of the NS method in this context is its ability to analyse a column as an integral part of the overall structure, rather than treating it as a separated element. This ability can have a significant impact in scenarios where there are significant irregularities in the structure or loading conditions.

In an attempt to retain the advantages of the NC method while extending its applicability to the assessment of column interactions with surrounding structural components, ConSteel has developed an approach that uses the global buckling configuration of the structure to determine the distribution of second-order bending moments more accurately. This paper attempts to compare three methods: the Eurocode 2 nominal curvature method (manual calculation), the ConSteel automatic nominal curvature method (aNC) and the GM method implemented within the ATENA software.

The nominal curvature method has faced criticism from researchers since its introduction in Eurocode 2 (EN 1992-1-1, 2004). Critics often highlight that the method yields conservative outcomes due to an overestimation of curvature in certain scenarios. Therefore, attempts were made to improve the precision of this method.

Barros (Barros et al., 2010) proposed an improved nominal curvature method, where the curvature is interpolated between the steel yield conditions and the maximum allowable curvature, depending on the axial load. For concrete classes above C60, the scenario in which both steel yields prevail is unattainable, resulting in a curvature being lower than the values prescribed in Eurocode 2.

Kollár, Csuka, and Ther (Kollár et al., 2014) remarked that concentrically loaded columns are not addressed in a distinct way. Eurocode introduces a "capacity reduction factor" for materials such as masonry, timber, and steel to facilitate calculations for concentrically loaded columns. Consequently, they have proposed formulae for determining the load-bearing capacity of such columns, claiming that their methodology is simpler and more precise than the simplified methods in Eurocode.

With the constant improvement of computational capacity, the general method can be seen as a valid alternative to improve accuracy. However, even if it is considered to be more accurate, its reliability is questionable. A primary concern is that stability failure can occur at reduced concrete stress and deformation (Fig. 1, right). In this context, due to the nonlinear stress-strain diagram inherent in the GM method, there is a reduced margin of safety compared to that when failure is due to concrete crushing. For stability failure, the dominant partial safety factor exerting influence is $\gamma_{CE}$, which reduces the Young's modulus of concrete. Alternatively, to more accurately address this issue, probabilistic analysis methods can be used, including the estimation method of coefficient of variation (ECOV), which have been proposed by researchers such as Wolinski (Wolinski, 2011) and Cervenka (Cervenka, 2013).

Dobry (Dobry et al., 2022) conducted laboratory experiments and developed numerical models to explore the probability of unsafe design consequences due to the use of the GM method. His findings indicated that employing the GM method absent laboratory test calibration culminates in a 47% disparity between the maximum and minimum buckling force. This is attributable to uncertainties related to material properties, dimensions, and nonlinear compressive structural behaviour. This uncertainty raises questions regarding the feasibility of using the GM method safely in design applications, necessitating the incorporation of additional safety measures in design contexts where GM methods are applied.

This confirms the premise that simplified methods are appropriate for practical routine design applications.

## 2. PROBLEM STATEMENT

The nominal curvature method does not precisely take into account the interaction of adjacent columns, which places the responsibility on the designer to correct the calculations when necessary. ConSteel's novel method, called the automatic nominal curvature method, claims to be able to handle this issue automatically, which can prevent designer errors. Detailed information on this method can be found in ConSteel's knowledge base article (ConSteel, 2023).

The main objective of this paper is to validate the ConSteel method and to further emphasise the possible errors that can occur during the design of irregular structural systems. Three distinct computational approaches were compared: (1) an analytical calculation in accordance with Eurocode 2, using the nominal curvature method; (2) finite element modelling within ConSteel, applying a novel approximation of second-order bending moments based on buckling shapes, described in the software as the 'automatic nominal curvature' method; (3) the general method using geometrically nonlinear analysis performed in the ATENA software. The three methods handle geometric nonlinearity and imperfections with different levels of precision. Further aim of this study is to show the effects of more precise considerations on the load bearing capacity of reinforced concrete columns.

**Fig. 1:** *Stability failure of slender columns (left), concrete stress-strain diagram with mean and design values (right) (Dobry et al., 2022)*

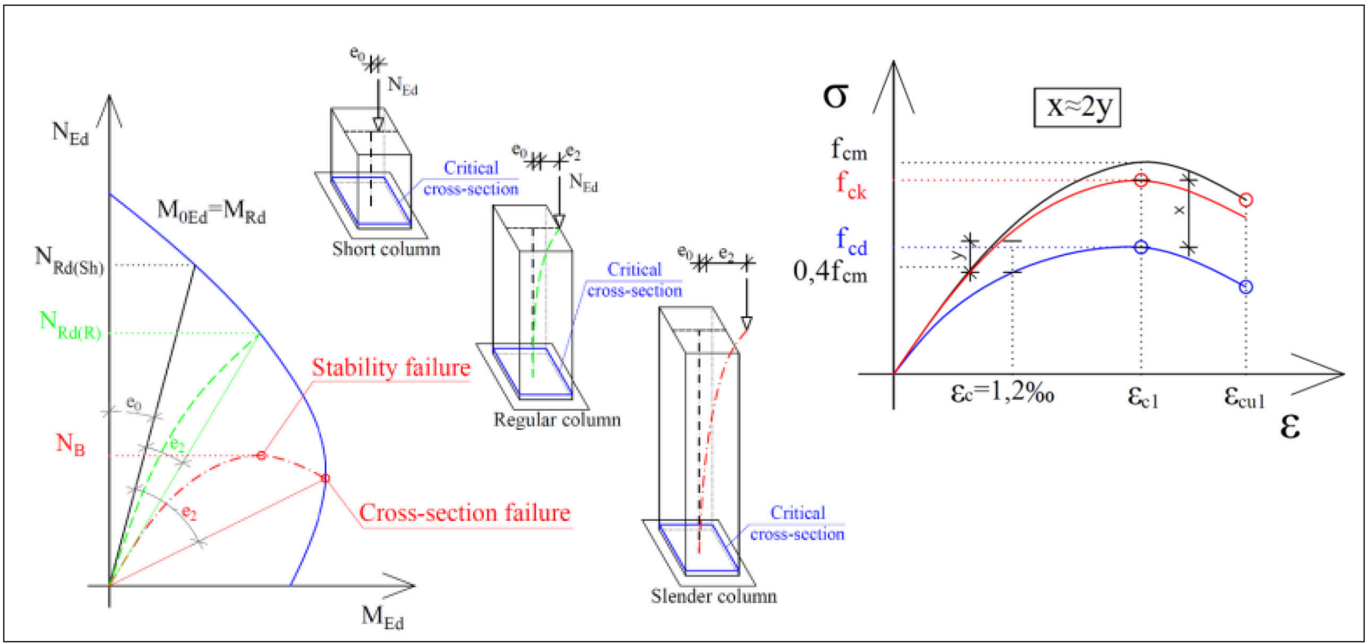

# 3. APPROACH

To investigate the problem, single columns under axial compression with different support conditions were first evaluated, followed by two columns connected by a stiff beam with hinged connections. The columns studied were either loaded at different intensities, had different boundary conditions, or had different cross-sectional areas.

An imperfection of 1/200 of the height of the columns was taken into account in all three calculations. In the case of the NC and aNC methods, this imperfection was taken into account with a horizontal load, whereas in the GM method the geometry was defined in an imperfect way. The distribution of the imperfection followed the buckling shape of the column (which was dependent on the boundary conditions) where the maximum intensity was equal to 1/200 of the height of the columns.

The effect of curvature was taken into account in the NC case by the second-order bending moment, with a uniform distribution, while in the aNC case, the distribution of the second-order bending moment was determined based on linear buckling analysis (LBA).). The GM method automatically considered the curvatures by geometrically nonlinear analysis.

In the NC case, a first-order analysis was sufficient, while in the aNC case a LBA and also a buckling sensitivity analysis was necessary. LBA is needed to calculate the distribution of the curvatures, and buckling sensitivity analysis is essential, since the software uses the results of this analysis to assign the correct buckling shapes for each column. In the aNC method, interaction between structural elements is taken into account by the LBA, whereas the GM method uses geometrically nonlinear analysis.

Creep in the NC and aNC methods is considered using the final value of the creep coefficient , to calculate factor , which is then used to calculate the curvature. In the GM method creep is considered in a simplified way, by using the effective design value of the Young's modulus of concrete (), where the final value of the creep coefficient is the same as previously used for the NC and aNC methods.

The maximum load bearing capacity of the columns for each problem was determined using the N-M biaxial bending interaction diagram for the NC and aNC methods, and by the maximum point of the load-displacement curve for the GM.

# 4. NUMERICAL MODELS

Initially, single column scenarios were tested. The simplicity of these cases allowed for the comparison of the three computational methods and the calibration of the parameters used. The objective was to obtain comparable results at failure under conditions of maximum loading and maximum curvature. The notation for each case and the boundary conditions are summarised in Table 1.

Having achieved similar results in three types of evaluation using single-column models, identical models were then used to construct two column frames. The apices of the columns were connected by a rigid beam, incorporating hinged connections, as shown in Fig. 2 (middle). The sole function of this element is to facilitate the transfer of loads between the two columns.

A comprehensive analysis was carried out that included five different cases. First, identical columns with fixed-free boundary conditions were subjected to equivalent loading intensities at the top. This approach was intended for validation purposes, and the expected result reflected the results obtained when testing single columns under similar boundary conditions. In the second scenario, the loading conditions were changed so that only one column was subjected to a load, while the adjoining column remained unloaded, but was subjected to lateral forces from the connected column. In the third scenario, both columns were loaded; however, one column was subjected to only half the load intensity. In the fourth scenario, the conditions were the same as in the first scenario, but the columns were designed with cross-sectional areas that provided a bending stiffness ratio of one to five between them. The final and fifth scenarios maintained the conditions of the first but introduced a variation in the support conditions: One column had a hinged bottom support, while the other column retained a fixed support. The notations for the two-column scenarios are summarised in Table 2.

## 4.1 Geometry

The columns considered in our calculations were each 6.00 metres high and had a cross-sectional area of 400 by 400 millimetres. The reinforcement specifications included a concrete cover of 3 centimetres, four longitudinal steel bars with a diameter of 28 millimetres and stirrups with a diameter of 10 millimetres, uniformly distributed at 200 millimetre intervals.

The geometry of the models is shown in Fig. 2. In models with different bending stiffness between the two columns, a ratio of 1:5 was achieved by reducing the dimensions of

**Table 1:** *Summary of single column calculation cases*

| Single columns | | | |
|---|---|---|---|
| Method | Notation | Bottom support | Top support |
| Eurocode 2: Nominal Curvature Method | NC_cant | fix | free |
| | NC_ss | hinged | hinged |
| | NC_bs | fix | hinged |
| ConSteel: Automatic Nominal Curvature Method | aNC_cant | fix | free |
| | aNC_ss | hinged | hinged |
| | aNC_bs | fix | hinged |
| Eurocode 2: General Method – ATENA | GM_cant | fix | free |
| | GM_ss | hinged | hinged |
| | GM_bs | fix | hinged |

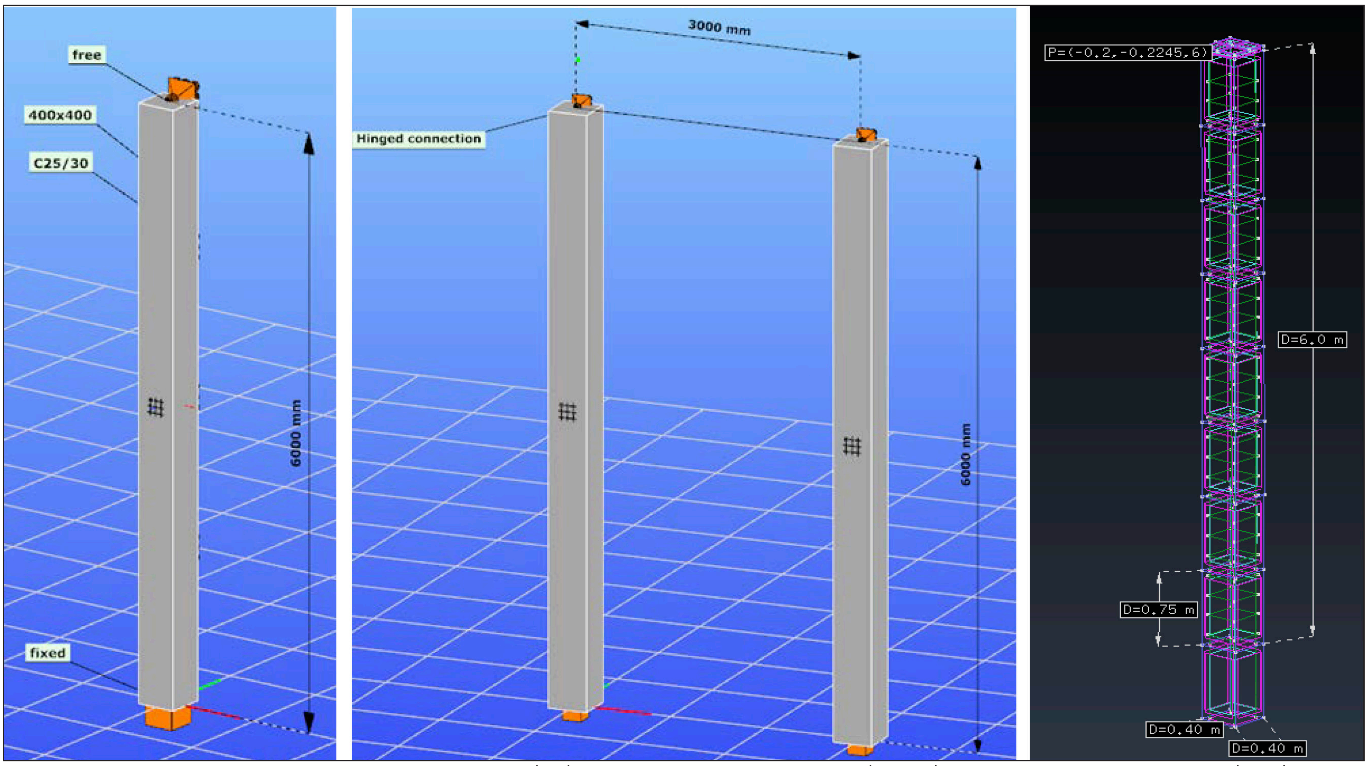


**Fig. 2:** Geometry of models: single cantilever in ConSteel (left), two-column frame in ConSteel (middle), and single cantilever in ATENA (right).

**Table 2:** Summary of two-column frame calculation cases

| Two-column frames | | |
|---|---|---|
| Method | Notation | Description |
| Eurocode 2: Nominal Curvature Method | NC_PP | Identical columns, identical loading. For model validation. |
| | NC_P0 | Identical columns, only one is loaded. |
| | NC_2PP | Identical columns, one column is loaded twice as much as the other one. |
| | NC_EI | Bending stiffness ratio between the columns is 1:5, identical loading. |
| | NC_SS | Identical columns, identical loading, one column is simply supported. |
| ConSteel: Automatic Nominal Curvature Method | aNC_PP | Identical columns, identical loading. For model validation. |
| | aNC_P0 | Identical columns, only one is loaded. |
| | aNC_2PP | Identical columns, one column is loaded twice as much as the other one. |
| | aNC_EI | Bending stiffness ratio between the columns is 1:5, identical loading. |
| | aNC_SS | Identical columns, identical loading, one column is simply supported. |
| Eurocode 2: General Method - ATENA | GM_PP | Identical columns, identical loading. For model validation. |
| | GM_P0 | Identical columns, only one is loaded. |
| | GM_2PP | Identical columns; one column is loaded twice as much as the other one. |
| | GM_EI | The bending stiffness ratio between the columns is 1:5, identical loading. |
| | GM_SS | Identical columns, identical loading; one column is simply supported. |

one column to 267.5×267.5 mm. Consequently, the inertia ratio of the columns is 1:5, while their modulus of elasticity remains constant. In the NC and aNC scenarios, columns were specified with ideal geometry, and imperfections were accounted for by horizontal loads (see Chapter 3.3). In the GM approach, it was necessary to model the structure with its imperfect geometry to conduct an imperfect analysis. The imperfect geometry followed the buckling shape of the column, where the largest displacement value was equal to 1/200 of the height of the column. In ATENA, solid elements were utilised for concrete, while so-called 1D bar elements were used for reinforcement. The centre line of the reinforcement bars was modelled. Additional plates were incorporated as volume elements for loading purposes. Anticipating failure in the cantilever column in the bottom section, the columns were extended to provide a continuous mesh at the base. The 6.00 m column was subdivided into eight sections, each 750 mm in length. Each square-based prism was offset by 1/8 of the imperfection value to form a parallelepiped. This was essential to ensure the accuracy of the model. The use of a curved line would have precluded the use of hexahedral elements for meshing. In instances involving two columns, the rigid beam was modelled as a solid steel beam that employs solid elements. This element had adequate stiffness and facilitated the definition of the necessary loads and connections.

## 4.2 Materials

In the calculations, C25/30 grade concrete and B500B reinforcement were used. The design for the modulus of elasticity of the concrete was used as specified:

$$E_{cd} = E_{cm}/\gamma_{cE}, \tag{1}$$

where  is the mean value of the modulus of elasticity, and is the partial safety factor for the modulus of elasticity of concrete.

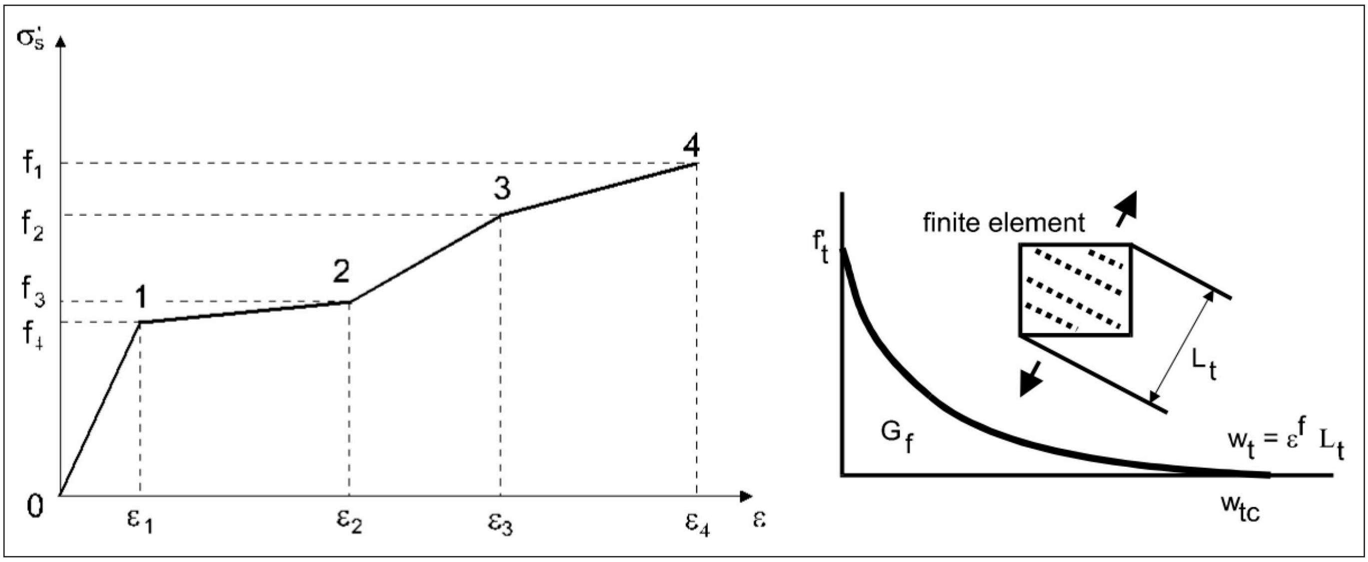

**Fig. 3:** *Multilinear stress-strain law (left), tensile softening, and characteristic length (right) (Cervenka et al., 2020)*

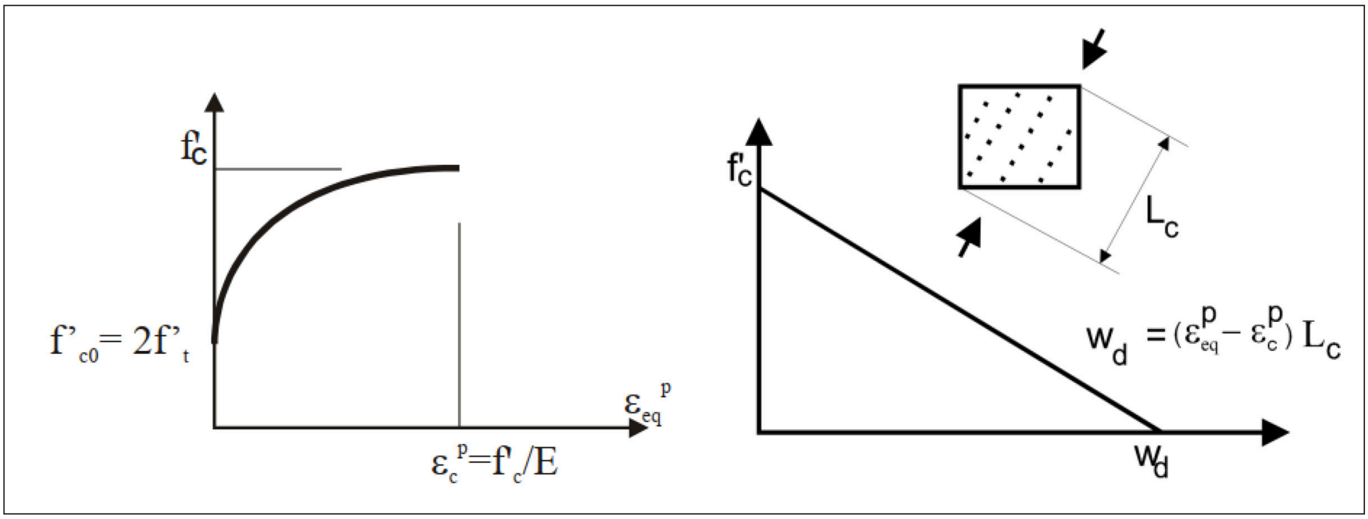

**Fig. 4:** *Compressive hardening/softening and compressive characteristic length. Based on experimental observations by Van Mier (Cervenka et al., 2020)*

In the NC and aNC scenarios, linear isotropic material models were used. In these cases, the consideration of creep in the calculations of the second-order bending moments negated the need for further modifications. The GM method was used to account for material nonlinearity. The multilinear stress-strain law was applied to the reinforcement as shown in Fig. 3 (left). This multilinear approach consists of four segments and facilitates the modelling of all four stages of steel behaviour: elastic state, yield plateau, hardening, and fracture. For B500B steel, a modulus of elasticity of 200 GPa and a design yield strength of 435 MPa were used.

In the study, the ATENA CC3DNonLinCementitous2 material model was used for the concrete analysis. This model integrates a fracture-plastic framework that combines constitutive approaches for tensile (fracture) and compressive (plastic) behaviours. The fracture mechanism is based on an orthotropic smeared crack formulation paired with a crack band model. It accommodates both the rotated and fixed crack models, and our analysis utilises the fixed crack model. As depicted in Fig. 3 (right), the size of the crack band, denoted $L_c$, is determined by projecting the size element in the direction of the crack. Fig. 4 illustrates the compressive behaviour, where the ascending (hardening) phase is characterised by an elliptical shape, while the descending (softening) phase follows a linear trajectory. The governing equation for the ascending branch is strain-based, whereas the descending branch is displacement-driven to address issues related to mesh size.

In our models, the interface between the concrete and the reinforcement is rigidly established, indicating the absence of slippage. The nodes associated with the one-dimensional elements are systematically generated to ensure alignment at the boundaries with the concrete elements.

To consider the effect of creep, the effective modulus of elasticity of concrete was used in GM models:

$$E_{\mathrm{cd,eff}} = \frac{E_{\mathrm{cm}}}{\gamma_{\mathrm{cE}}\left(1+\varphi(\infty,t_0)\right)}, \tag{2}$$

where is the same value as later used in Consteel calculations (for curvature).

## 4.3. Boundary Conditions

In the examination of planar scenarios, all models are supported in the y direction, while the x-z plane is under investigation. To establish a fixed column end in the GM method, support was defined on the lower surface of the 6.00 metre column in the x, y and z directions. To create a hinge between the solid steel beam and the top loading plate, only the centreline of the loading surface was connected to the

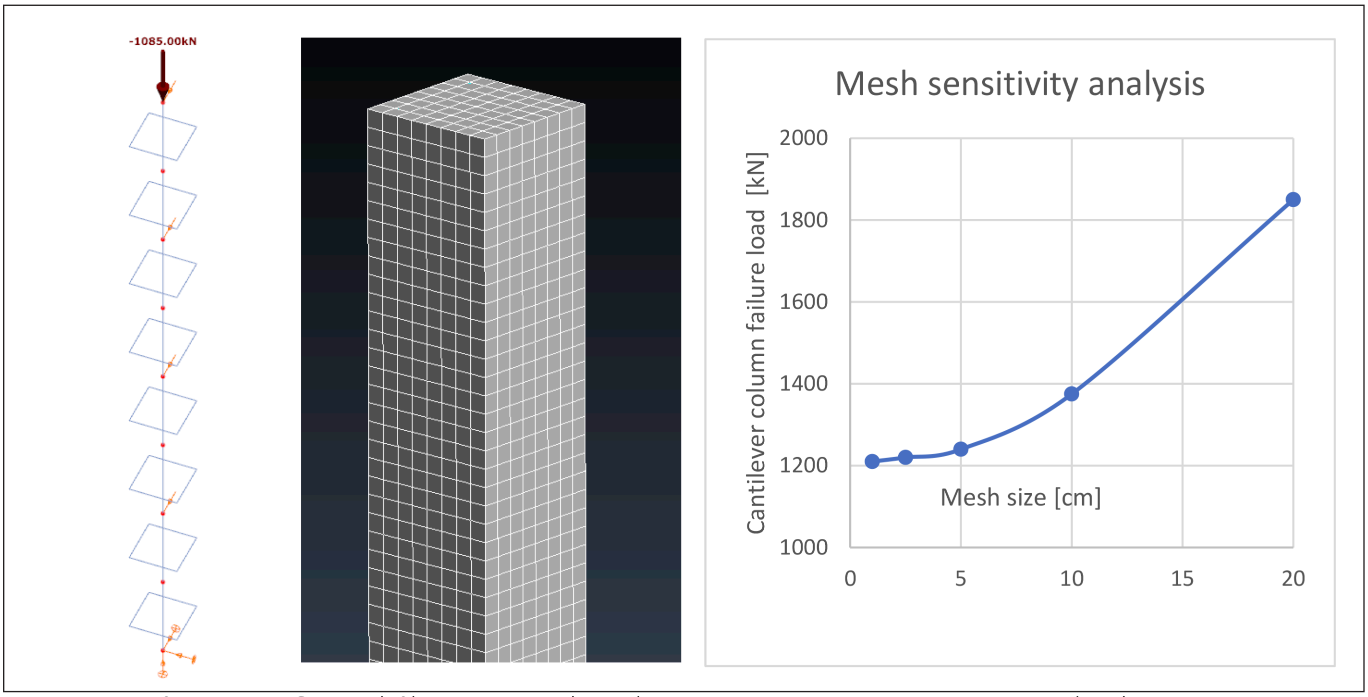


**Fig. 5:** Meshing for: models in ConSteel (left), ATENA models (middle), Mesh sensitivity analysis on cantilever column (right)

steel beam. Vertical loads were applied axially to the top of the columns, ignoring the self-weight. In both the NC and aNC cases, horizontal loads were characterised by a 1/200 imperfection (using the height of the column). The magnitude of the vertical loads increased progressively in all scenarios, until structural failure occurred, as indicated by the crushing of the concrete (see Chapter 3.5). In ConSteel, the support conditions were specified using the point support function.

## 4.4 Mesh

For the aNC models, the automatic mesh size suggested by ConSteel was utilised, resulting in the formation of elements measuring 75 cm in length with the software employing 8 meshes. The GM models incorporated hexahedral elements with an edge length of 5 cm. This dimension was derived from the mesh sensitivity analysis (Fig. 5 on the right) conducted on the single cantilever column, where mesh sizes ranging from 1 to 20 cm were examined. A 5 cm mesh size was selected because it yielded a discrepancy of less than 1% compared to the converged failure load.

## 4.5 Analysis parameters

Several analyses had to be performed in order to handle the aNC cases. First-order, buckling, and buckling sensitivity analyses were performed. It was imperative to verify the corresponding buckling modes assigned to the columns. Through the employment of the GM methodology, a Geometrically and Materially Nonlinear Imperfect Analysis (GMNIA) was intended. Imperfections were incorporated in the geometric definition as outlined in Chapter 3.1, while material nonlinearity was addressed as per the explanation in Chapter 3.2. Nonlinear analysis was conducted using the Arc-Length method, which was favoured over the Newton-Raphson method due to its suitability for load-controlled numerical experiments. This method also facilitated the investigation of the descending branch of the phenomenon. The Elastic Predictor was employed to compute between iterations, whereas the Pardiso solver was used for matrix solutions. A load increment of 10 kN was applied. Under these conditions, satisfactory mathematical convergence was achieved, with most iterative steps converging in under ten iterations. However, as the failure load was approached, an increase in the number of iterations was observed.

# 5. RESULTS

An evaluation was carried out on three main characteristics. Initially, the curvature and the second-order bending moments were examined to acquire a comprehensive understanding of the behaviour. Subsequently, the failure modes of the columns were analysed along with the identification of the specific column that failed. Ultimately, the failure load associated with the various methodologies and cases was systematically compared.

## 5.1 Curvature

A comprehensive visualisation of the curvatures is presented in the Appendix. A single figure, comprising three sub-figures for each column, has been developed. The figure on the left figure shows the numerical curvature data for the three calculation types: NC, aNC, and GM. The central figure depicts the second-order bending moment diagram for the corresponding column, derived from the aNC method. The configuration of this diagram is determined solely by the structural buckling shape. The right figure demonstrates the results of the GM method, which include either the complete bending moment diagram or the axial stress state within the column. This diagram is generated by integrating the stresses of the column member. The analysis of individual column cases revealed a robust concordance with both curvature values and shapes. The second-order bending moment diagram shows a similar configuration using both the aNC and GM methods, reinforcing the postulation that the buckling shape provides a valid assumption for the second-order bending moment distribution.

*P-0 and 2P-P cases*

The analysis of the two-column frame cases gives interesting results. In the P-0 scenario, two main phenomena can be observed. Firstly, the unloaded column exhibits a second-order bending moment. This is due to the top-level lateral action exerted by the adjacent column, which results in a linear second-order bending moment. It could be argued that the unloaded column provides "support" to the loaded one. Secondly, the interaction between the columns causes an upward shift in the maximum value of the second-order bending moment within the loaded column. This change is confirmed by both the aNC and GM methods. The disparity in curvature for the loaded column is attributed to the primary failure of the unloaded column which occurred in a stress controlled manner. An analogous effect is observed in the 2P-P scenario. However, the difference is that the second-order bending moment is nonlinear due to the simultaneous loading of the other column. The maximum curvature and second-order bending moment for the P-loaded column are located at the base, and this effect shifts upward for the 2P-loaded column.

*Fix-hinged and EI case*

The fixed-hinged scenario is notable for the requirement that the fixed column must bear the bending moments imparted on both columns. On the contrary, the hinged column is limited to accommodating compressive forces. The application of the aNC method induces a minimal bending moment on this column, due to its inherent buckling configuration. Although this is not essential, it does not introduce any inaccuracies. Similarly, in the EI scenario, the column exhibiting the higher stiffness will bear a larger portion of the loads. It will also assume part of the bending moments of the less rigid column, thereby providing support to this weaker column. This interaction leads to a pronounced upward shift in the curvature and second-order bending moment diagram for the softer column.

## 5.2 Failure mode

When examining the single-column cases, it is clear that there is no significant difference between the methods in terms of failure modes. In the relatively slender cantilever column scenario, a balanced failure mode was observed, that is, when the concrete reached its ultimate compressive strain, the tensioned bars simultaneously reached their yielding strain. As illustrated in Fig. 6 (left), this represents the maximum bending moment point on the N-M bending interaction diagram.

Regarding the less slender simply supported and fixed-hinged columns, a compression-controlled failure mode was observed, indicating that the tensioned reinforcements remained elastic during the concrete crushing process. The failure modes for each calculation are presented systematically in Table 3. Within NC calculations, due to its focus on isolated columns, an identical failure mode was consistently identified across all calculations, invariably resulting in the failure of the weaker, less stiff, and more heavily loaded column. However, this does not fully encompass the complexities observed in real-world scenarios.

Upon examining the interaction between the columns, certain cases initially yielded unforeseen results. Specifically, when only one of the columns was subjected to loading, it was unexpected to observe the failure of the unloaded column. As the unloaded column was devoid of compression forces, the occurrence of a second-order moment was not anticipated. Nevertheless, due to its connection with the loaded column, second-order moments were indeed present in the unloaded column, as described in Chapter 4.1.

The unloaded column has a reduced bending moment capacity compared to the loaded column. Due to the interaction, second-order bending moments manifest in this column, resulting in a tension-controlled failure mode (see Fig. 7 left). A similar phenomenon is observed when one column bears half the load compared to the other column. This column has a reduced normal force and reduced bending moment capacity compared to the more extensively loaded column. In accordance with the Nominal Curvature method, the second-order bending moment should also be lower. However, due to the interaction with the other column, the second-order bending moment becomes more pronounced for the column with lesser loading, when juxtaposed with calculations performed independently, as delineated in Chapter 4.1. This interaction precipitates a tension-controlled failure in the lesser loaded column prior to the failure of the column subjected to double the load.

When one column is fixed and the other is hinged, only

**Table 3:** Summary of failure modes

| | NC | | aNC | | GM |
|---|---|---|---|---|---|
| Case | Failure mode | Utilization of the other column [%] | Failure mode | Utilisation of the other column [%] | Failure mode |
| cant | Balanced | - | Balanced | - | Balanced |
| ss | Compression controlled | - | Compression controlled | - | Compression controlled |
| bs | Compression controlled | - | Compression controlled | - | Compression-controlled |
| PP | Balanced | 100 | Balanced | 100 | Balanced |
| P0 | Loaded column - balanced | 0 | Unloaded column - tension controlled | 60 | Unloaded column - tension controlled |
| 2PP | 2P loaded column - balanced | 53 | P-loaded column - tension controlled | 89 | 2P column - tension controlled |
| EI | Less stiff column - balanced | 26 | Stiffer column - tension controlled | 44 | Buckling |
| SS | Fix column - balanced | 50 | Fix column - tension controlled | 16 | Fix column - tension controlled - buckling |

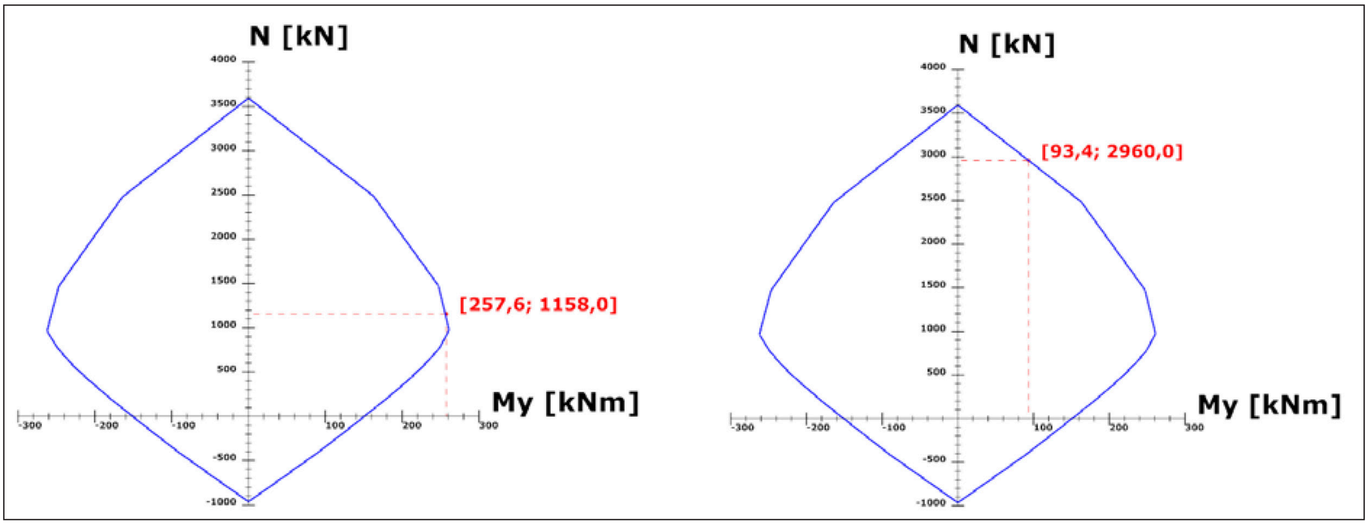


**Fig. 6:** N-M bending interaction diagram: for aNC_cant (left) and for aNC_ss (right)

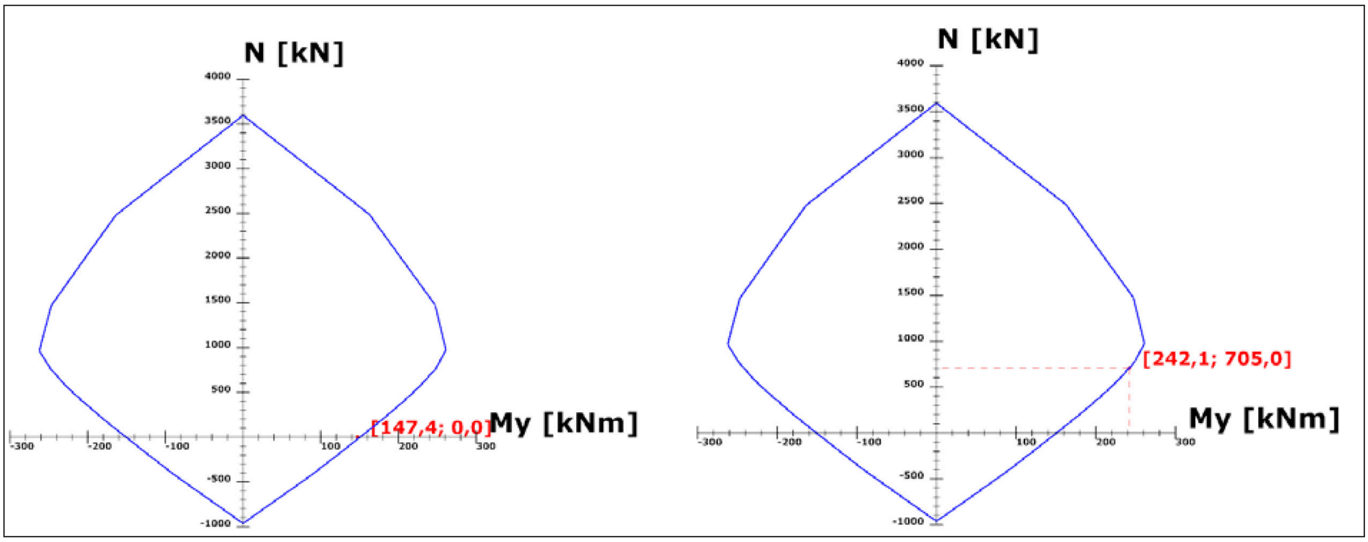


**Fig. 7:** N-M bending interaction diagram: for aNC_P0: unloaded column (left), and for aNC_2PP: P loaded column (right).

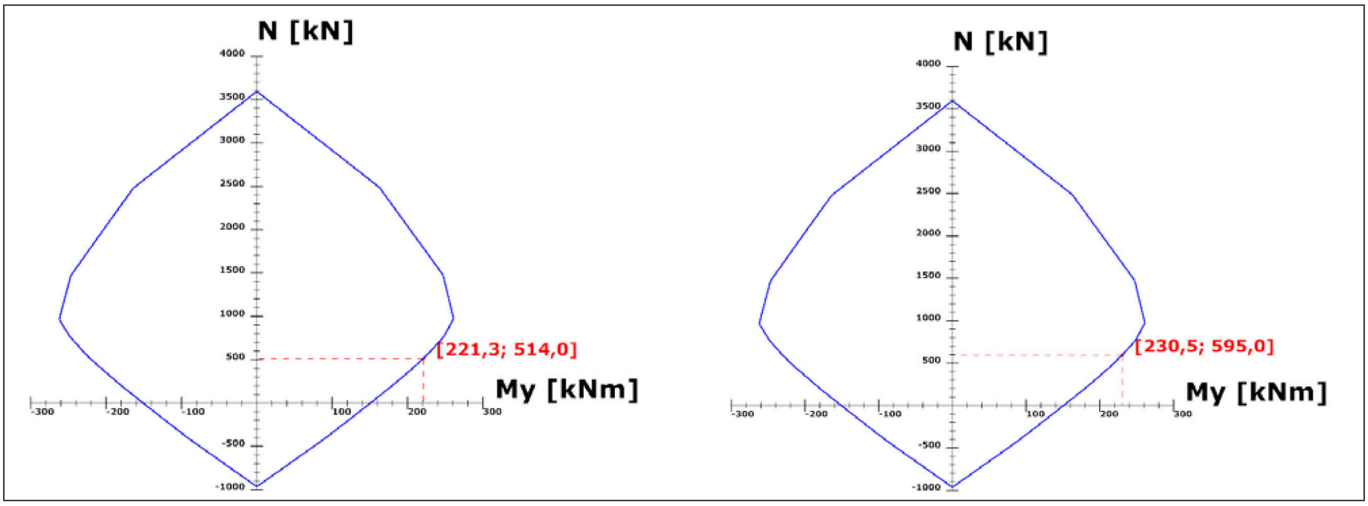


**Fig. 8:** N-M bending interaction diagram: for aNC_SS: fixed column (left), and for aNC_EI: stiffer column (right)

the fixed column will experience bending moments. If the interaction between the columns is not considered, the scenario is similar to a single cantilever column. However, the inclusion of the interaction results in a tension-controlled failure mode that occurs sooner. This is attributed to the fixed column having to withstand the horizontal loads applicable to both columns. As discussed in Chapter 4.1, this results in significantly increased second-order bending moments for the fixed column. A similar phenomenon is observed when the stiffness of one column exceeds that of the other. The Nominal Curvature method predicts the failure of the softer column first. However, with interaction is considered, the stiffer column provides support to the softer column, thereby shifting the failure to the stiffer one due to increased second-order bending moments (see Fig. 8 right).

## 5.3 Failure load

Table 4 shows the failure loads relevant to the calculations. As explained in Chapters 4.1 and 4.2, there is no significant variation in the calculations for a single column. The

**Table 4:** Summary of Failure Loads

| | GM | NC | | aNC | |
|---|---|---|---|---|---|
| Case | Failure load [kN] | Failure load [kN] | Difference [%] | Failure load [kN] | Difference [%] |
| cant | 1200 | 1158 | -3,5 | 1158 | -3,5 |
| ss | 2885 | 2960 | 2,6 | 2960 | 2,6 |
| bs | 3350 | 3250 | -3,0 | 3270 | -2,4 |
| PP | 1200 | 1158 | -3,5 | 1158 | -3,5 |
| P0 | 1380 | 1158 | -16,1 | 1300 | -5,8 |
| 2PP | 1635 | 1158 | -29,2 | 1410 | -13,8 |
| EI | 667 | 292 | -56,2 | 595 | -10,8 |
| SS | 592 | 1158 | 95,6 | 514 | -13,2 |

NC method consistently evaluates isolated elements; consequently, so the failure load of the cantilever column is always 1158 kN. Within the EI model, this load is reduced due to the reduced cross-sectional area. However, the interaction between the columns is completely ignored. In the P-0 and 2P-P scenarios, the failure load is increased in the aNC method and further increased in the GM method, due to the mutual support among the elements. Specifically, in the P-0 context, the unloaded column underpins the loaded one, thus improving its resistance. The increase is limited to 1300 kN, as the unloaded column collapses in a tension-controlled mode. When the alternate column is subjected to half the load, its bending capacity increases, culminating in an increase in the failure load from 1300 kN to 1410 kN in the aNC method and from 1380 kN to 1635 kN in the GM method. In the EI scenario, the failure load increases significantly when the intercolumn interaction is considered, increasing from 292 kN (NC) to 595 kN for the aNC method and to 667 kN for the GM method. Here, the stiffer member provides support to the less rigid column. In all scenarios examined, the interaction resulted in an increased failure load, thereby making the NC method conservative. In contrast, in the SS scenario, the failure load is reduced by half because one column has to support the bending loads of two columns. As the NC method considers an isolated column, this effect is completely overlooked. Although this situation is relatively atypical, it serves as a warning to be more careful when neglecting the interaction between columns.

# 6. CONCLUSIONS

The role of connected member on the load bearing capacity of compressed reinforced concrete columns was investigated using different calculation methods. Manual calculations were performed according to the nominal curvature method of Eurocode 2, and the automatic nominal curvature method developed in ConSteel was also applied. Furthermore, the general method according to Eurocode 2 was implemented in the ATENA software using nonlinear analysis. To find the differences between the methods, single columns under axial compression with different support conditions were first evaluated, followed by two columns connected by a stiff beam with hinged connections. The columns studied were either loaded at different intensities, had different boundary conditions, or had different cross-sectional areas.

The general method was used as a basis for a more precise consideration of imperfections and geometrical nonlinearity. Our investigation has shown that the nominal curvature method disregards column interaction, which is conservative in most cases. In particular cases, an increase in load on a column, due to the necessity to support substantial loads transferred from other columns, either because one column is more rigid, or because a column is unable to resist horizontal loads, results in the inability of the nominal curvature method to accurately represent the behaviour. This limitation can lead to underdesign and compromise safety. However, the novel approach of the ConSteel software, called the automatic nominal curvature method, which utilises buckling shapes to calculate the distribution of curvatures, was shown to be able to automatically consider the interaction between concrete columns, preventing serious errors from occurring in the case of irregular structural systems.

The effect of creep in this study was taken into account in a simplified manner, further research is needed to better understand its effect on the load bearing capacity of compressed concrete columns. Also the novel method developed in ConSteel should be further studied in order to find more problems where this solution could be applied.

To construct structures that are both safer and more cost-effective, it is essential to account for the interaction among structural elements. Various approaches exist to achieve this, ranging from simplified modelling techniques to the more advanced general method. Ultimately, it is up to the designer's judgement to determine the appropriate solution for the specific problem.

# 7. ACKNOWLEDGEMENTS

The authors extend their profound gratitude to Professor László Kollár for his invaluable guidance. His conceptual insights on structural analysis were indispensable to this study. Acknowledgements are also due to ConSteel Solutions Kft. for providing a licence, facilitating our exploration of the software's functionalities. We are equally appreciative of Červenka Consulting s.r.o. for their assistance with the general methodology, with particular thanks to Jiří Rymeš for his expertise in meshing and result evaluation.

Project no. BME-380 has been implemented with the support provided by the Ministry of Culture and Innovation of Hungary from the National Research, Development and Innovation Fund, financed under the EKÖP-24-3 funding scheme.

EKÖP

The project was also supported by the Doctoral Excellence Fellowship Programme (DCEP) is funded by the National Research Development and Innovation Fund of the Ministry of Culture and Innovation and the Budapest University of Technology and Economics, under a grant agreement with the National Research, Development and Innovation Office.

## 8. REFERENCES

EN 1992-1-1-2004. *Eurocode 2: Design of Concrete Structures-Part 1-1: General Rules for Buildings*., 2004

de Araújo, J. M. (2017). „Comparative study of the simplified methods of Eurocode 2 for second-order analysis of slender reinforced concrete columns.” *Journal of Building Engineering*, 14, 55–60, Nov. 2017, doi: https://doi.org/10.1016/j.jobe.2017.10.003

Barros, H., Silva, V.D., & Ferreira, C. (2010). „Second-order effects in slender concrete columns-reformulation of the Eurocode 2 method based on nominal curvature.” *Engineering Structures*, 32(12), 3989–3993, Dec. 2010, doi: https://doi.org/10.1016/j.engstruct.2010.08.005

Kollár, L.P., Csuka, B., & Ther, T. (2014). „Simplified design of concentrically loaded reinforced concrete columns,” *The Structural Engineer: journal of the Institution of Structural Engineer*, 92, 48–56, 2014

Woliński, S. (2011). „Global Safety Factor or Nonlinear Design of Concrete Structures,” *Archives of Civil Engineering*, 57, 331-339, Sep. 2011, doi: https://doi.org/10.2478/v.10169-011-0023-3

Cervenka, V. (2013). „Global safety formats in fib Model Code 2010 for design of concrete structures”, *Proceedings of the 11th International Probabilistic Workshop*, Brno, 2013

Dobrý, J., Wolfger, H. & Benko, V. (2022). „Reliability of slender concrete columns designed according to the Eurocodes,” *Engineering Structures*, 265, 114266, Aug. 2022, doi: https://doi.org/10.1016/j.engstruct.2022.114266

Cervenka, V., Jendele, L., & Cervenka, J. (2020). „Theory,” *in ATENA Program Documentation Part 1*, Sep. 2020

Consteel, (2023). „Reinforced concrete columns – applying the Automatic Nominal Curvature Method for design”. https://consteelsoftware.com/knowledgebase/reinforced-concrete-columns-applying-the-automatic-nominal-curvature-method-for-design

**Szabolcs Szinvai** (1997) MSc structural engineer at Budapest University of Technology and Economics. currently pursuing his PhD studies at Department of Structural Engineering, Budapest University of Technology and Economics. Research fields: Embedded FRP reinforcement in concrete structures, focusing on bond and the structural behaviour. A member of the Hungarian group of *fib*, head of the Hungarian *fib* Young Member group and involved in TG10.3 “Examples for Model Code” in *fib*. szinvaiszab@edu.bme.hu

**Bálint Vaszilievits-Sömjén** (????) Head of R&D Group of Consteel, responsible for the coordination of development of new software features, research tasks. Preparation of webinars and keep international contact with partners involved in Consteel development. balint.vaszilievits-somjen@keszgroup.com

**Tamás Kovács** (1974) Associate Professor at Budapest University of Technology and Economics, Department of Structural Engineering. Research areas: damage analysis of concrete structures based on dynamic characteristics, high performance concretes for bridges, concrete pavements, reliability of structures. kovacs.tamas@emk.bme.hu

## APPENDIX: CURVATURES

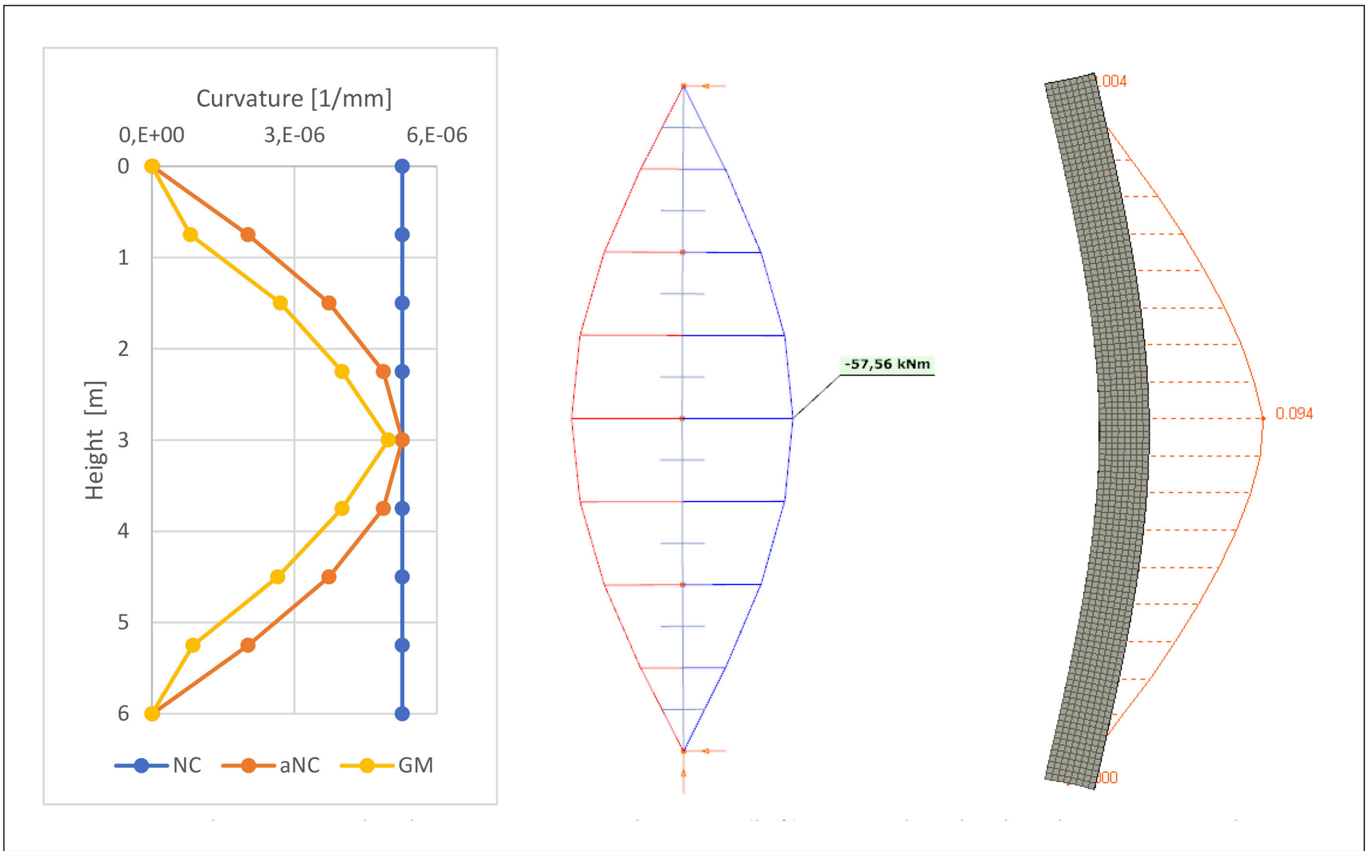


**Fig. 9:** Simply supported column: curvature diagram (left), second-order bending moment diagram for aNC (middle) and bending moment diagram for GM [MNm] (right)

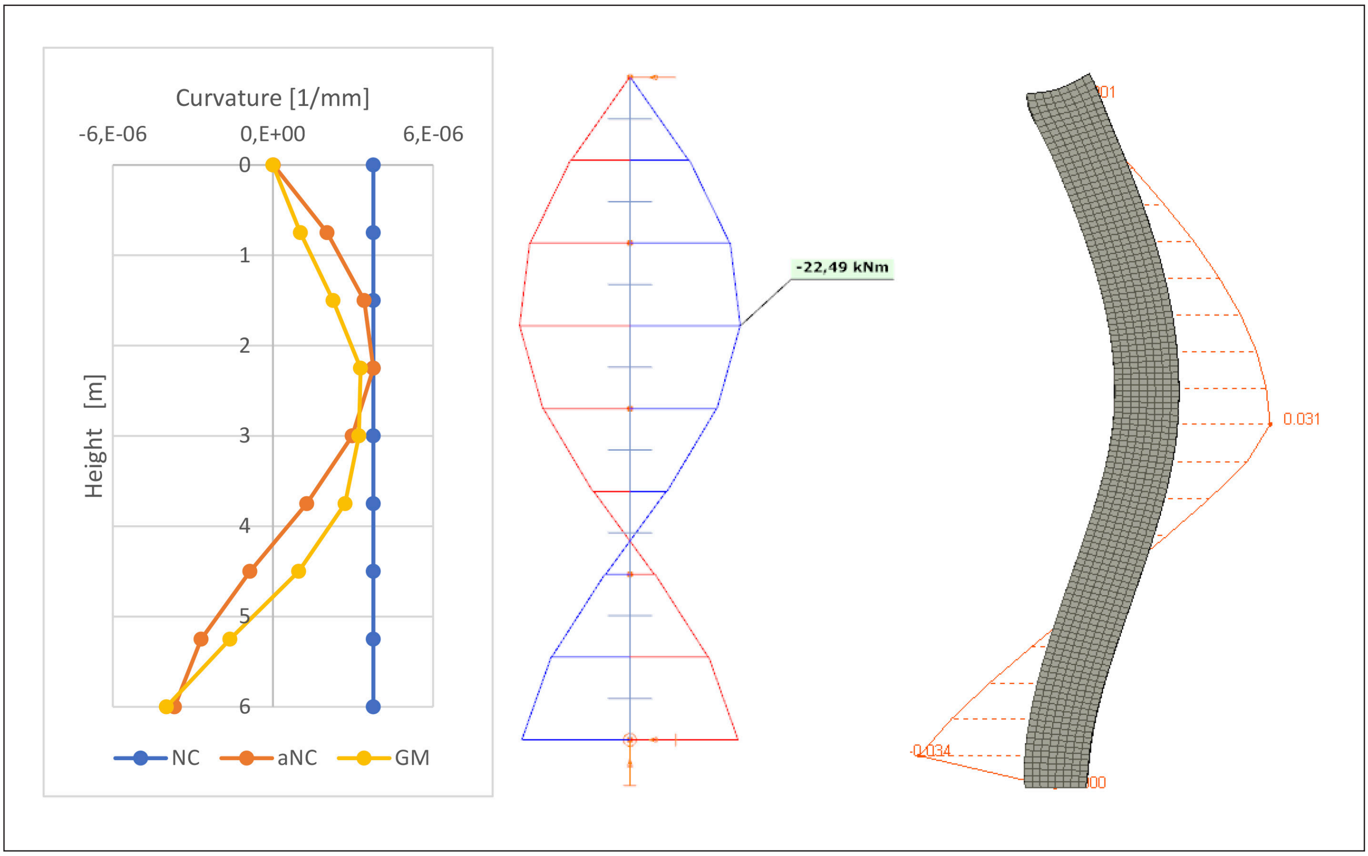


**Fig. 10:** Fix-hinged column: curvature diagram (left), second-order bending moment diagram for aNC (middle) and bending moment diagram for GM [MNm] (right)

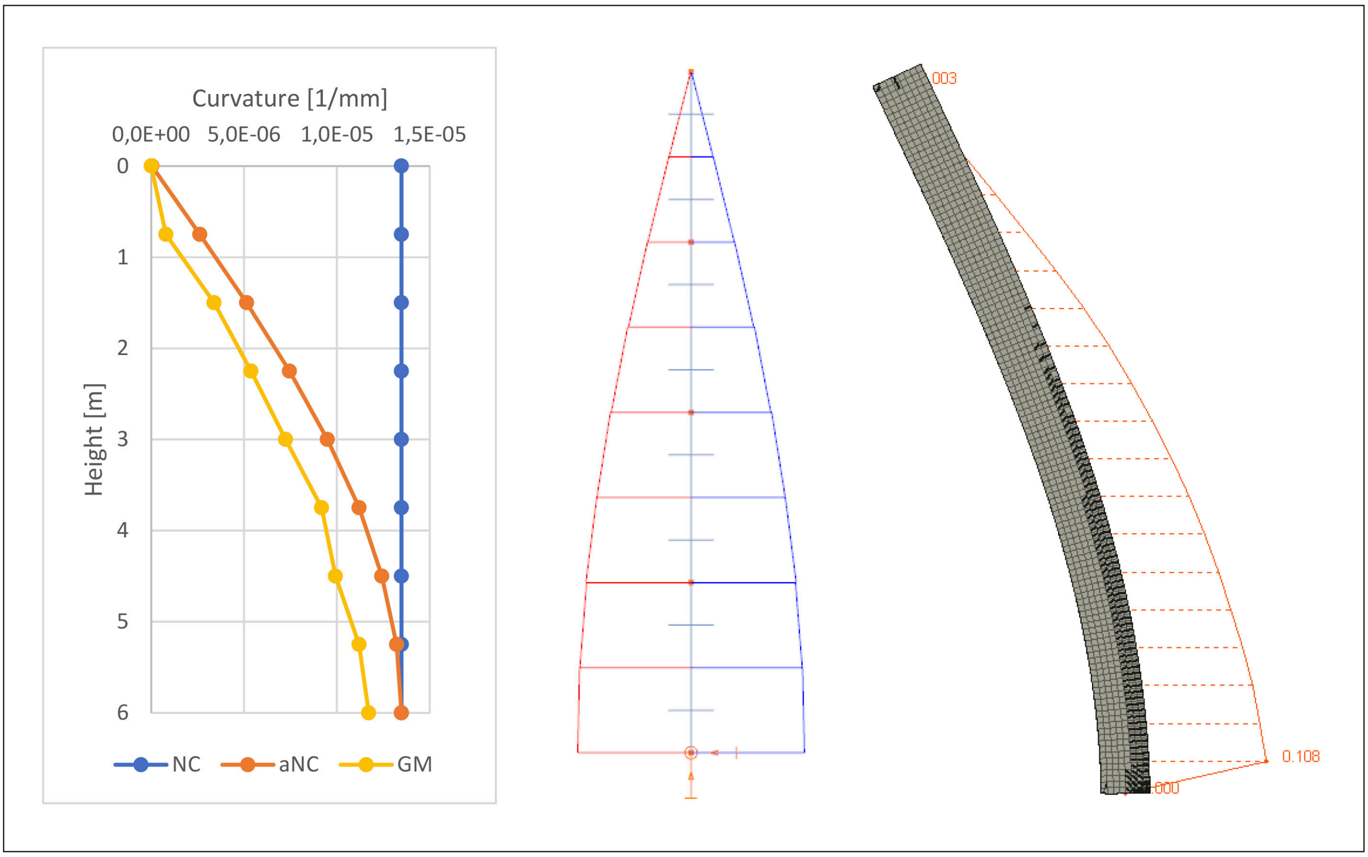


**Fig. 11:** Simply supported column: curvature diagram (left), second-order bending moment diagram for aNC (middle) and bending moment diagram for GM [MNm] (right)

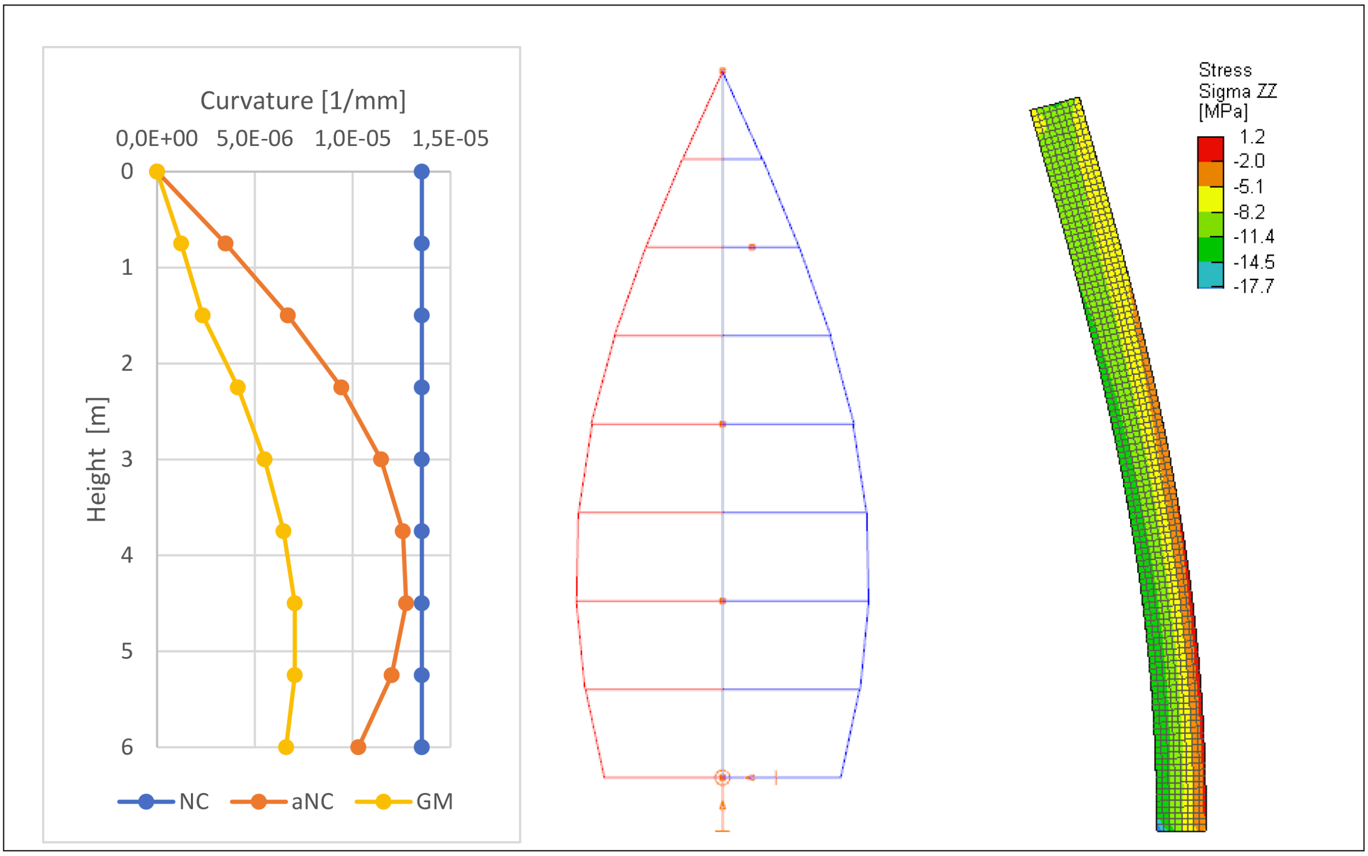


**Fig. 12:** P-0 case, P loaded column: curvature diagram (left), second-order bending moment diagram for aNC (middle) and stresses for GM [MNm] (right)

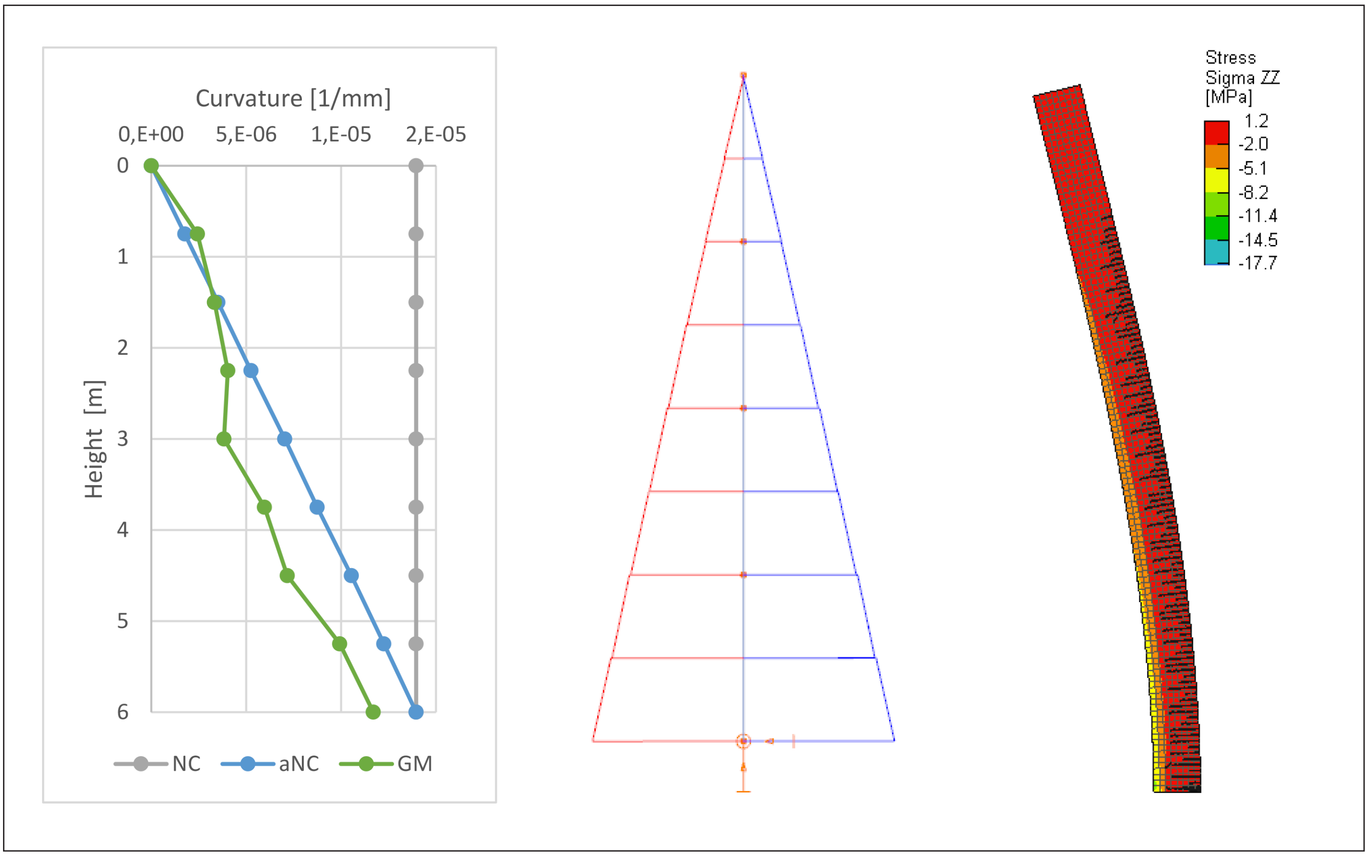


**Fig. 13:** P-0 case, unloaded column: curvature diagram (left), second-order bending moment diagram for aNC (middle) and stresses for GM [MNm] (right)

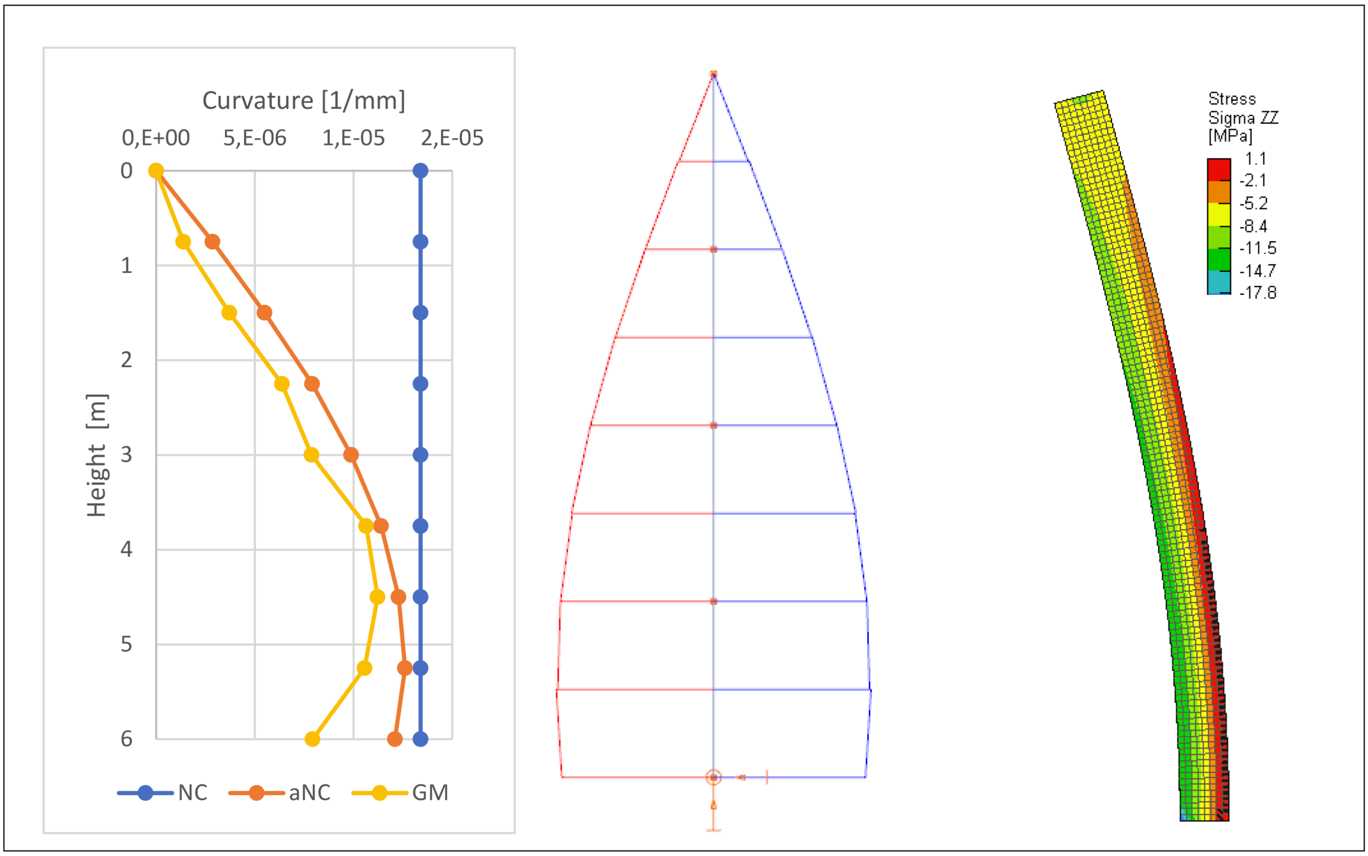


**Fig. 14:** 2P-P case, 2P loaded column: curvature diagram (left), second-order bending moment diagram for aNC (middle) and stresses for GM [MNm] (right)

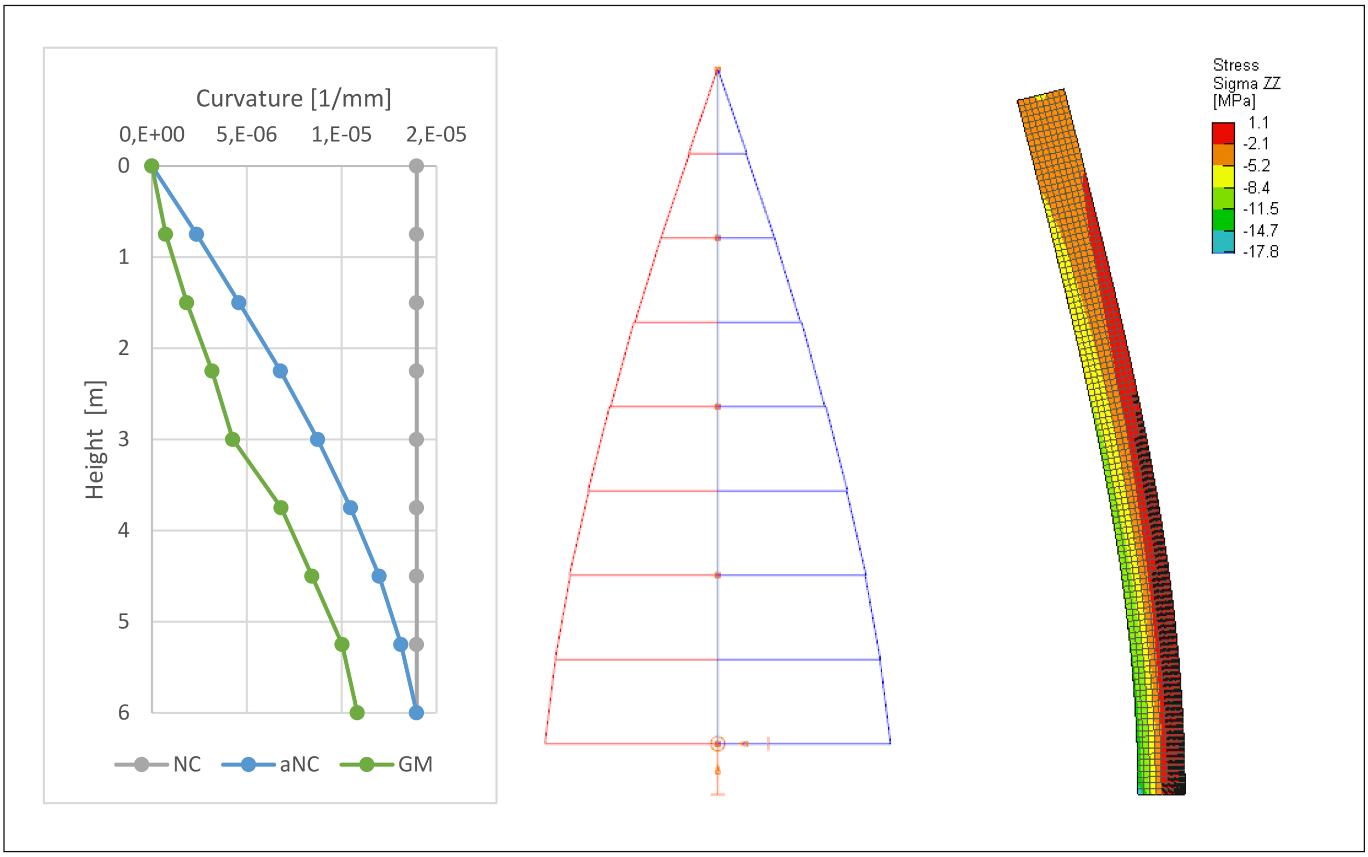


**Fig. 15:** 2P-P case, P loaded column: curvature diagram (left), second-order bending moment diagram for aNC (middle) and stresses for GM [MNm] (right)

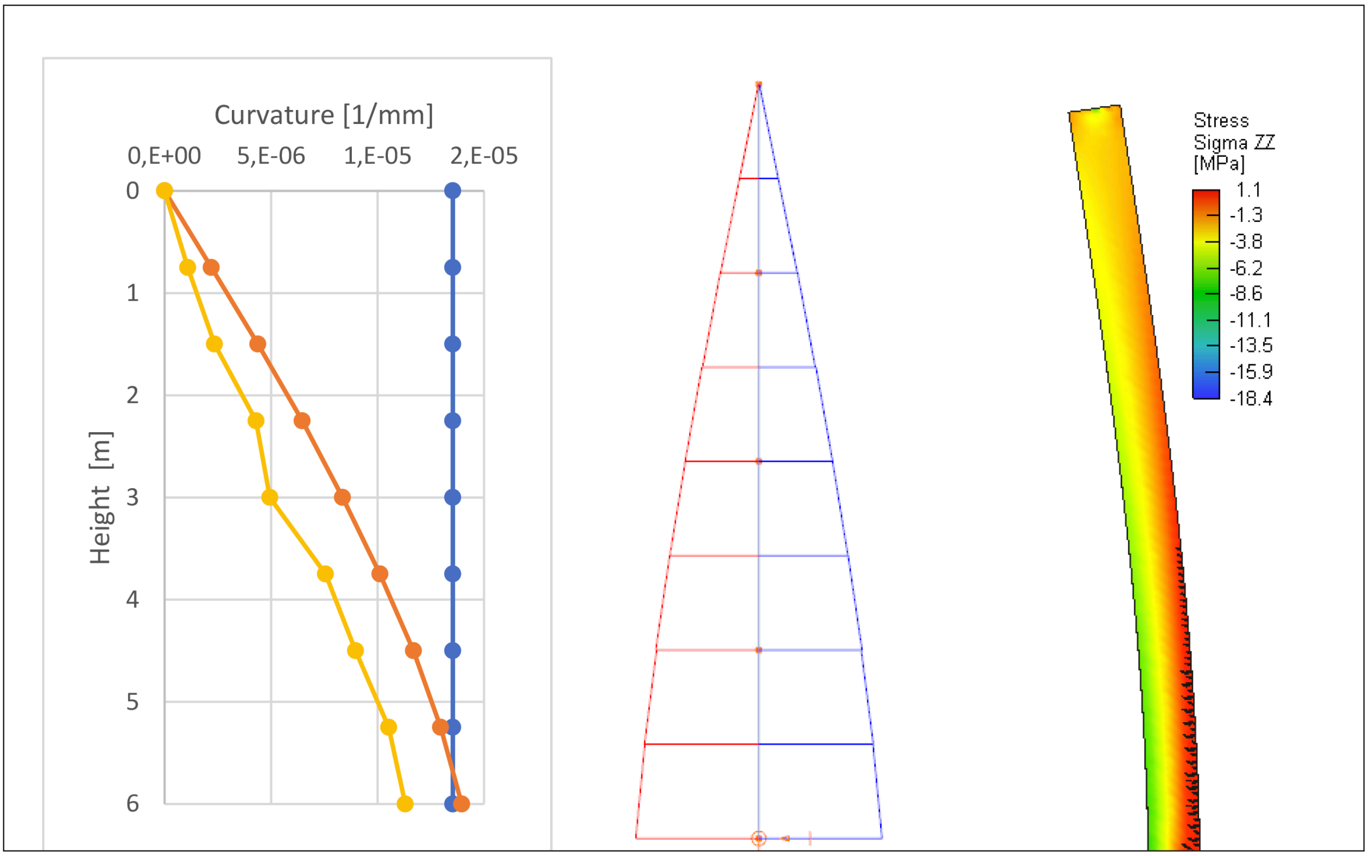


**Fig. 16:** Fix-hinged, fix column: curvature diagram (left), second-order bending moment diagram for aNC (middle) and stresses for GM [MNm] (right)

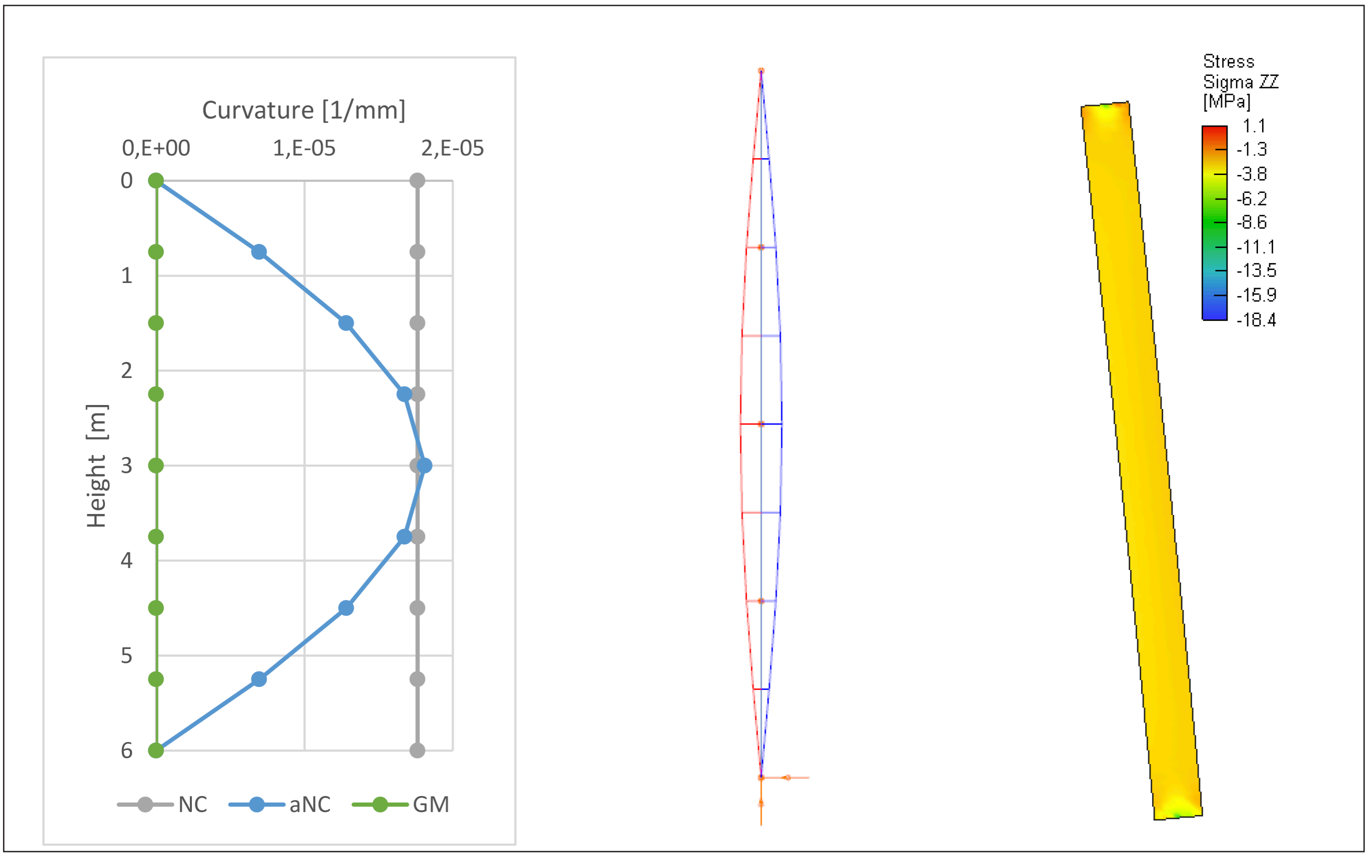


**Fig. 17:** Fix-hinged, hinged column: curvature diagram (left), second-order bending moment diagram for aNC (middle) and stresses for GM [MNm] (right)

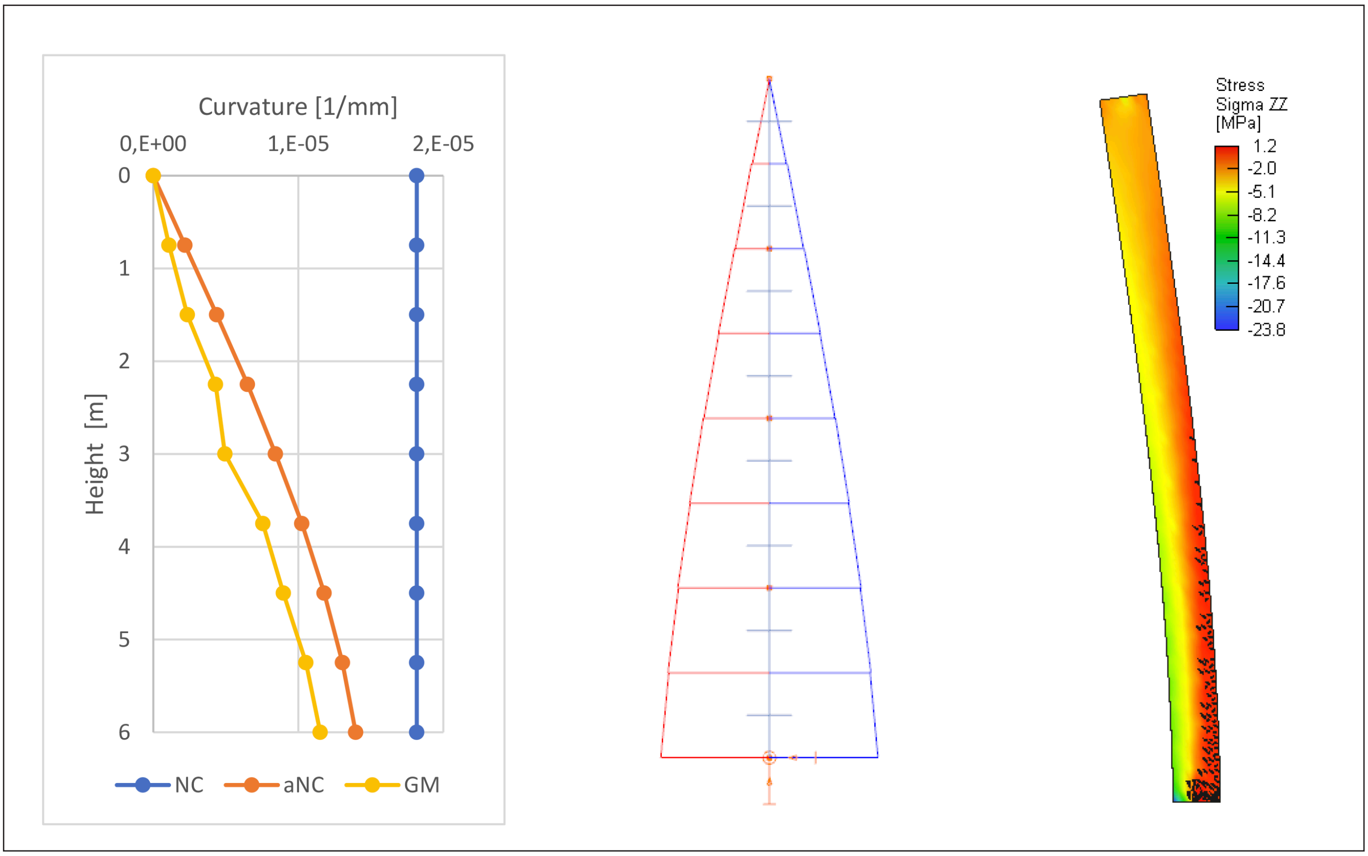


**Fig. 18:** EI, stiffer column: curvature diagram (left), second-order bending moment diagram for aNC (middle) and stresses for GM [MNm] (right)

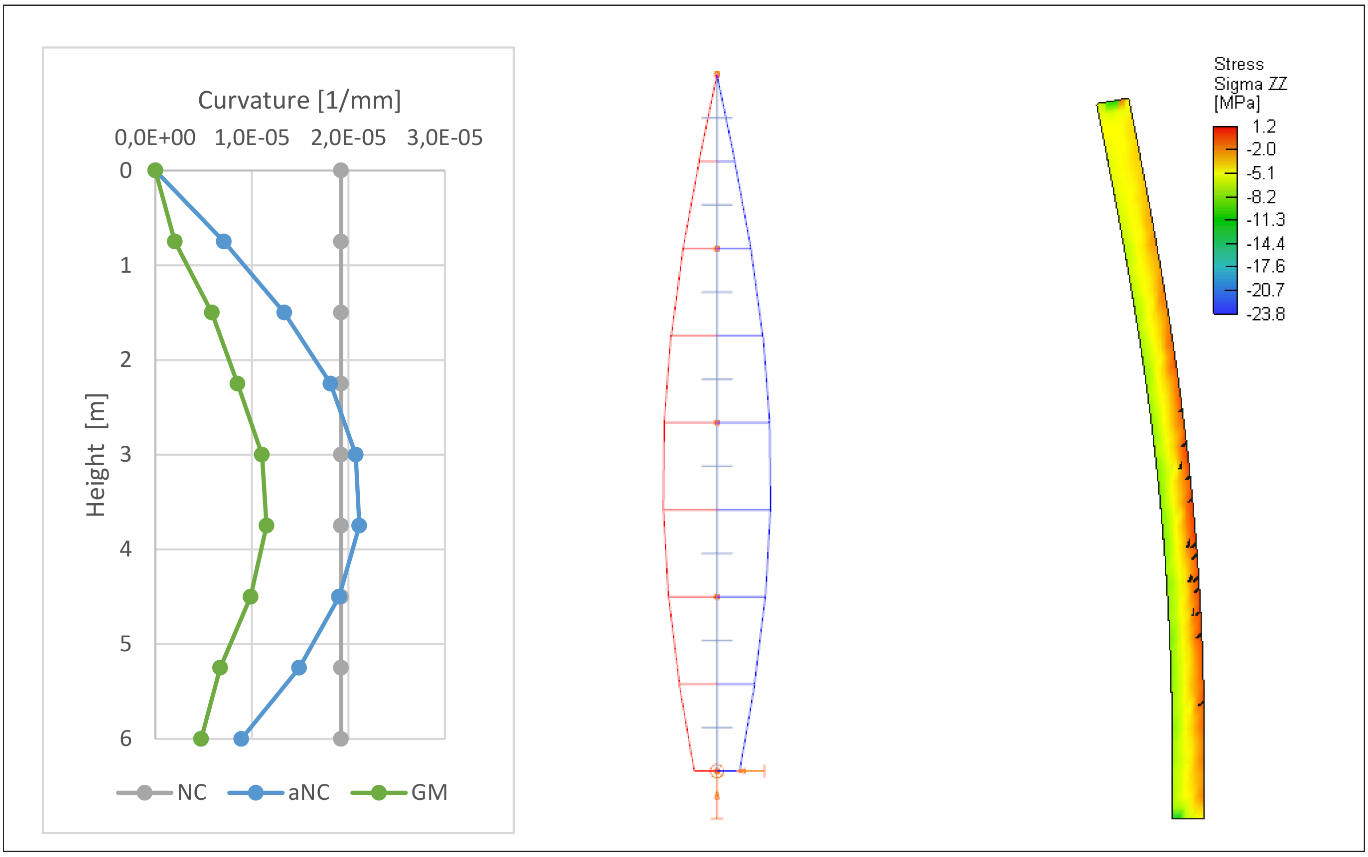


**Fig. 19:** EI, softer column: curvature diagram (left), second-order bending moment diagram for aNC (middle) and stresses for GM [MNm] (right)